Article

J. Biol. Regul. Homeost. Agents. 2024; 38(7): 5463–5471
https://doi.org/10.23812/j.biol.regul.homeost.agents.20243807.438

Heparanase Inhibitor OGT2115 Alleviates Myocardial Hypoxia/Reoxygenation Injury in H9c2 Cells through the MAPK/ERK Pathway

Haiyan Lin[1], Ying Zhou[2], Da Gao[1], Guangze Xu[1], Yifei Xu[3,*]

[1]Department of Cardiology, Ningbo Medical Center Lihuili Hospital, 315000 Ningbo, Zhejiang, China
[2]Department of Cardiology, Zhejiang Provincial People's Hospital, People's Hospital of Hangzhou Medical College, 310014 Hangzhou, Zhejiang, China
[3]Department of Cardiology, First Affiliated Hospital of Zhejiang Chinese Medical University, 310006 Hangzhou, Zhejiang, China
*Correspondence: yifeixudoc@163.com (Yifei Xu)
Submitted: 23 August 2022 Revised: 9 October 2022 Accepted: 24 November 2022 Published: 1 July 2024

Background: Heparanase (HPSE) is an endo-beta-D-glucuronidase, and its upregulation is associated with many inflammatory diseases, such as atherosclerosis, fibrosis, and cancer. However, the role of HPSE in myocardial infarction remains unclear.
Methods: Cell Counting Kit-8 (CCK8) assay was used to detect the development of the oxygen-glucose deprivation/reoxygenation (OGD/R) model and the effect of HPSE inhibitor OGT2115. Real-time quantitative PCR (RT-qPCR) and western blotting were used to detect HSPE expression in OGD/R model, the effect of HPSE inhibitor OGT2115, and the expression of cell proliferation-related protein, apoptosis-related protein, and fibrosis-related protein. The immunofluorescence assay was used to detect the expression of 5-Ethynyl-2′-Deoxyuridine (EdU) and TdT-mediated dUTP nick-end labeling (TUNEL). Enzyme-linked immunosorbent assay (ELISA) assay was used to detect the secretion of cytokines associated with the OGD/R model.
Results: HPSE was highly expressed in the OGD/R model, and its inhibitor OGT2115 significantly promoted the proliferation and inhibited the apoptosis and fibrosis of H9C2 cells in the OGD/R model. Simultaneously, OGT2115 inhibited the secretion of inflammatory factors—tumor necrosis factor-α (TNF-α), interleukin-6 (IL-6), and IL-8—in the OGD/R model. Further mechanistic studies demonstrated that OGT2115 could inhibit the phosphorylation of mitogen-activated protein kinases (MAPK) and extracellular signal-regulated kinase (ERK).
Conclusion: HPSE inhibitor OGT2115 alleviates myocardial IR injury in H9c2 cells and inhibits the MAPK/ERK pathway, indicating that HPSE is crucial in regulating myocardial infarction, and its inhibitor OGT2115 may be a potential drug for the treatment of myocardial infarction.

Keywords: heparanase; myocardial infarction; oxygen-glucose deprivation/reoxygenation model; OGT2115; MAPK/ERK

Introduction

Cardiovascular disease kills more people annually than any other cause of death, making it the leading global cause [1]. Myocardial infarction (MI) is a cardiovascular and cerebrovascular disease that seriously endangers human health [2]. Myocardial infarction refers to the ischemic necrosis of the myocardium. As coronary artery disease severely reduces or interrupts coronary blood flow, the associated myocardium experiences chronic acute ischemia, leading to ischemic myocardial necrosis [3]. As the population ages, the incidence of myocardial infarction increases. Even though improved medicine and MI reperfusion treatments can alleviate clinical symptoms and save lives [4], these treatments cannot fundamentally stop or halt the spread of heart failure following MI.

The best treatment for MI is currently myocardial reperfusion with thrombolysis or percutaneous coronary intervention [5]. Reperfusion, however, results in a further injury—known as myocardial ischemia/reperfusion (MI/R) injury. MI/R damage influences the final myocardial infarct size—a key predictor of prognosis in MI patients [6]. MI/R injuries can be difficult to treat clinically. It is believed that cardiomyocyte necrosis and apoptosis play essential roles in developing MI/R damage [7]. Following MI/R, numerous pathophysiological variables, including inflammation, oxidative stress, and fibrosis, are responsible for cardiomyocyte apoptosis [8]. Therefore, it is essential to develop innovative methods for reducing heart failure and post-MI remodeling.

Heparan sulfate (HS) is broken down by a single functional heparanase (HPSE) in mammalian cells, which facilitates the degradation of the extracellular matrix and releases effector molecules bound to HS [9]. HPSE can regulate various biological responses of cells, including cell proliferation, apoptosis, inflammation, angiogenesis, and cell migration [10]. Its dysregulation can lead to diabetes [11], tumors [12], and fibrotic diseases [13]. However, the func-

Journal of
BIOLOGICAL REGULATORS
and Homeostatic Agents

tion of HPSE in MI and its underlying mechanism remain unknown. OGT2115 is a potent, cell-permeable, orally active HPSE inhibitor [14]. OGT2115 was evaluated using a modified HS/bFGF 96-well plate assay for high-throughput screening of a library of 50,000 compounds with moderate cell-based anti-angiogenic activity. Therefore, the role of OGT2115 in MI was tested.

The present study investigated the role of HPSE in MI/R injury and its specific mechanism. We demonstrated for the first time that the inhibition of HPSE with OGT2115 could inhibit oxygen-glucose deprivation/reoxygenation (OGD/R)-induced mitogen-activated protein kinases (MAPK)/extracellular signal-regulated kinase (ERK) pathway activation, promote cell proliferation, and inhibit OGD/R-induced apoptosis, fibrosis, and inflammatory responses to attenuate MI/R injury. Our study suggests that inhibiting HPSE may be a therapeutic approach for treating heart failure.

Materials and Methods

Establishment of a Model for OGD/R Injury in H9c2 Cells

H9c2 cells (4201RAT-CCTCC00606) were obtained from the Institute of Biochemistry and Cell Biology of the Chinese Academy of Sciences. The cells were grown in a 37 °C incubator with 10% FBS, 100% air, 5% CO_2, 100 mg/mL streptomycin, and 100 U/mL penicillin. The medium was changed every two to three days. PCR was frequently used to check cells for mycoplasma.

To construct the OGD/R model [15], we transferred the cells to an anoxic incubator: 1% O_2, 94% N_2, and 5% CO_2 (sugar-free medium), cultured for 2 h, and then immediately replaced with the normal medium and reoxygenated for 12 h.

Cell-Proliferation Assays

The cells (3×10^3) were grown for 48 h in the DMEM medium with 10% FBS and the corresponding agonists or inhibitors. OGT2115 (HY-100898, MCE, Shanghai, China) was configured to a storage concentration of 10 mM dissolved in DMSO. The desired concentration was diluted with the culture medium before each use. The Cell Counting Kit-8 (CCK8) test (A311, Vazyme, Nanjing, China) was used according to the manufacturer's instructions to measure the absorbance of each well at 450 nm (A450) using a multifunctional enzyme label (Infinite® 200 PRO, Tecan, Männedorf, Switzerland).

Western Blot Assay

The cells were lysed with RIPA buffer and protease inhibitor (A32963, Thermo Scientific, San Jose, CA, USA), and the cells were then centrifuged at 13,000 g for 20 min. Protein lysates were separated using SDS/PAGE, blotted onto a PVDF membrane, and probed overnight at 4 °C with the following antibodies: mouse anti-glyceraldehyde-3-phosphate dehydrogenase (GAPDH) (1:5000; sc-32233, Santa Cruz Biotechnology, Santa Cruz, CA, USA), mouse anti-HPSE (1:1000, ab85543, Abcam, Boston, MA, USA), mouse anti-CDK1 (1:500, 9116, CST, Boston, MA, USA), mouse anti-PCNA (1:1000, sc-56, Santa Cruz Biotechnology, Santa Cruz, CA, USA), rabbit anti-cleaved caspase-3 (1:1000, ab2302, Abcam, Boston, MA, USA), rabbit anti-LC3 (1:1000, 12741, CST, Boston, MA, USA), mouse anti-transforming growth factor β1 (TGF-β1) (1:1000, ab64715, Abcam, Boston, MA, USA), mouse anti-Col4 (1:500, ab6311, Abcam, Boston, MA, USA), rabbit anti-fibronectin (FN) (1:1000, ab2413, Abcam, Boston, MA, USA), rabbit anti-p38 MAPK (1:1000, 9212, CST, Boston, MA, USA), rabbit anti-p-p38 MAPK (1:1000, 9211, CST, Boston, MA, USA), rabbit anti-ERK1/2 (1:1000, 9102, CST, Boston, MA, USA), and rabbit anti-p-ERK1/2 (1:1000, 9101, CST, Boston, MA, USA). Thermo Fisher's goat anti-mouse or anti-rabbit IgG was used as the secondary antibody to probe stripped membranes, which were then detected using enhanced chemiluminescence with a Bio-Rad ChemiDoc™ exposure machine (Bio-Rad Laboratories, Inc., Hercules, CA, USA). Each protein band was quantified using Image J1 (Image J 150b, NIH, Bethesda, MD, USA), and the grayscale values were normalized to its corresponding internal reference protein, GAPDH, and labeled under the strips.

Real-Time Quantitative PCR (RT-qPCR) Assay

Trizol and the cDNA Synthesis Kit were used to extract and reverse-transcribe total RNA (R312, Vazyme, Nanjing, China). SYBR Green PCR Master Mix (Q311, Vazyme, Nanjing, China) was used in qPCR experiments with Roche LC480, and relative mRNA expression was adjusted to *GAPDH*. The $2^{-(\Delta\Delta Ct)}$ technique was used to analyze the results. The primers for *HPSE* were 5′-GCACAAACACTGACAATCCAAG-3′ and 5′-AAAAGGATAGGGTAACCGCAA-3′. The primers for *GAPDH* were 5′-GTGGTCTCCTCTGACTTCAACA-3′ and 5′-CCACCACCCTGTTGCTGTAG-3′.

Enzyme-Linked Immunosorbent Assay (ELISA)

Human tumor necrosis factor-α (TNF-α), interleukin-6 (IL-6), and IL-8 ELISA kits (ab181421, ab178013, ab214030, Abcam, Boston, MA, USA) were used to measure the levels of TNF-α, IL-6, and IL-8 in the cell culture supernatant. All steps were performed following the manufacturer's instructions. The absorbance of every well was detected using a multifunctional enzyme label (Infinite® 200 PRO, Tecan, Männedorf, Switzerland).

5-Ethynyl-2′-Deoxyuridine (EdU) Assay

The EdU kits (C10337, Thermo Scientific, San Jose, CA, USA) were used to perform EdU assays. The cells were co-cultured with EdU working solution (1:1000) for

2–4 h at 37 °C in a humidified 5% CO_2 environment. The cells were treated for 30 min with 0.3% Triton X-100 after being fixed for 30 min with 4% paraformaldehyde at room temperature. The cells were treated with the click response solution for 30 min at room temperature and in the dark, per the manufacturer's instructions, before being exposed to Hoechst solution for 10 min. Images were captured using a fluorescent microscope with a 200× magnification, and cell counts were performed using ImageJ1 software (Image J 150b, NIH, Bethesda, MD, USA).

TUNEL Assay

TdT-mediated dUTP nick-end labeling (TUNEL) Assay Kit - FITC was obtained from Abcam (ab66108). Following a 15 min fixative treatment with 1% paraformaldehyde, the cells were washed in PBS. Following the application of 70% ethanol, the cells were rinsed with buffer, incubated on ice for 30 min, and then added 50 µL of DNA labeling solution. The cells were then incubated for an additional hour at 37 °C. The cells were cultured for 30 min at low light before being suspended in propidium iodide (PI) solution and washed with buffer. The cells were then examined using a fluorescence microscope (BX53, Olympus, Tokyo, Japan).

Statistics

In this study, GraphPad 9.0 (GraphPad, Bethesda, MD, USA) was used for data analysis. All of the data included in this investigation represented at least three separate studies. The results are shown as means ± SD. The one- or two-way ANOVA and the two-tailed Student's *t*-test were evaluated for independent samples. The symbols *, **, ***, and **** indicate p values below 0.05, 0.01, 0.001, and 0.0001, respectively. p values < 0.05 were considered statistically different.

Results

HPSE was Highly Expressed in the OGD/R Model

First, we established an OGD/R injury model of H9c2 cells and tested the cell viability using the CCK8 assay to verify whether the cell model was established successfully. The CCK8 assay results demonstrated that the cell viability of H9c2 cells in the OGD/R injury model was significantly decreased compared with that in the normal group (Fig. 1A). Subsequently, we examined the mRNA and protein levels of HPSE in the OGD/R injury model. The RT-qPCR experiments revealed that the *HPSE* mRNA level of H9c2 cells in the OGD/R injury model was significantly up-regulated compared with that in the normal group (Fig. 1B). The WB experiments demonstrated that the HPSE protein level of H9c2 cells in the OGD/R injury model was significantly up-regulated compared with that in the normal group (Fig. 1C,D). The aforementioned experiments revealed that HPSE was highly expressed in the OGD/R injury model.

The HPSE Inhibitor OGT2115 Significantly Promoted the Proliferation of H9c2 Cells in the OGD/R Model

Subsequently, we applied different concentrations of HPSE inhibitor OGT2115 to examine the effect of HPSE on cell proliferation in the OGD/R injury model. First, the inhibition of HPSE expression in the cells by OGT2115 was detected using WB and RT-qPCR experiments (Fig. 2A–C). The inhibitory effect of OGT2115 on HPSE in H9c2 cells was concentration-dependent. The CCK8 assay results demonstrated that OGT2115 attenuated the inhibitory effect of the OGD/R injury model on cell viability, and the higher the concentration, the stronger the effect (Fig. 2D). We also detected the protein levels of pro-proliferative proteins CDK1 and PCNA. We found that the OGD/R injury model drastically reduced the expression of PCNA and CDK1. After the administration of OGT2115, their expression levels were significantly increased in a concentration-dependent manner (Fig. 2E–G). Finally, we examined the effect of OGT2115 on cell proliferation using immunofluorescence staining experiments with the proliferation marker EdU. OGD/R injury model significantly inhibited cell proliferation, whereas OGT2115 significantly promoted cell proliferation in the OGD/R injury model in a concentration-dependent manner (Fig. 2H,I). In conclusion, the HPSE inhibitor OGT2115 significantly promoted cell proliferation in the OGD/R injury model.

The HPSE Inhibitor OGT2115 Significantly Inhibited the Apoptosis and Fibrosis of H9c2 Cells in the OGD/R Model

We then examined the effect of OGT2115 on apoptosis and fibrosis in the OGD/R injury model. The WB results revealed that the expressions of pro-apoptotic proteins Caspase 3 and LC3 were significantly increased in the OGD/R injury model. After administration of OGT2115, their expression levels were significantly decreased in a concentration-dependent manner (Fig. 3A–C). The apoptosis marker TUNEL immunofluorescence staining demonstrated that the OGD/R injury model significantly promoted cell apoptosis. Simultaneously, OGT2115 significantly inhibited cell apoptosis in the OGD/R injury model in a concentration-dependent manner (Fig. 3C,D). The OGD/R injury model often causes cellular fibrosis. Therefore, we detected the expression of cellular fibrosis-related proteins collagen IV (Col-4), fibronectin (FN), and TGF-β1. The WB experiments revealed that the expression of collagen IV, fibronectin, and TGF-β1 were significantly increased in the OGD/R injury model. After administration of OGT2115, their expression levels were significantly decreased in a concentration-dependent manner (Fig. 3E,F). In conclusion, the HPSE inhibitor OGT2115 significantly inhibited apoptosis and fibrosis in the OGD/R injury model.

Journal of
BIOLOGICAL REGULATORS
and Homeostatic Agents

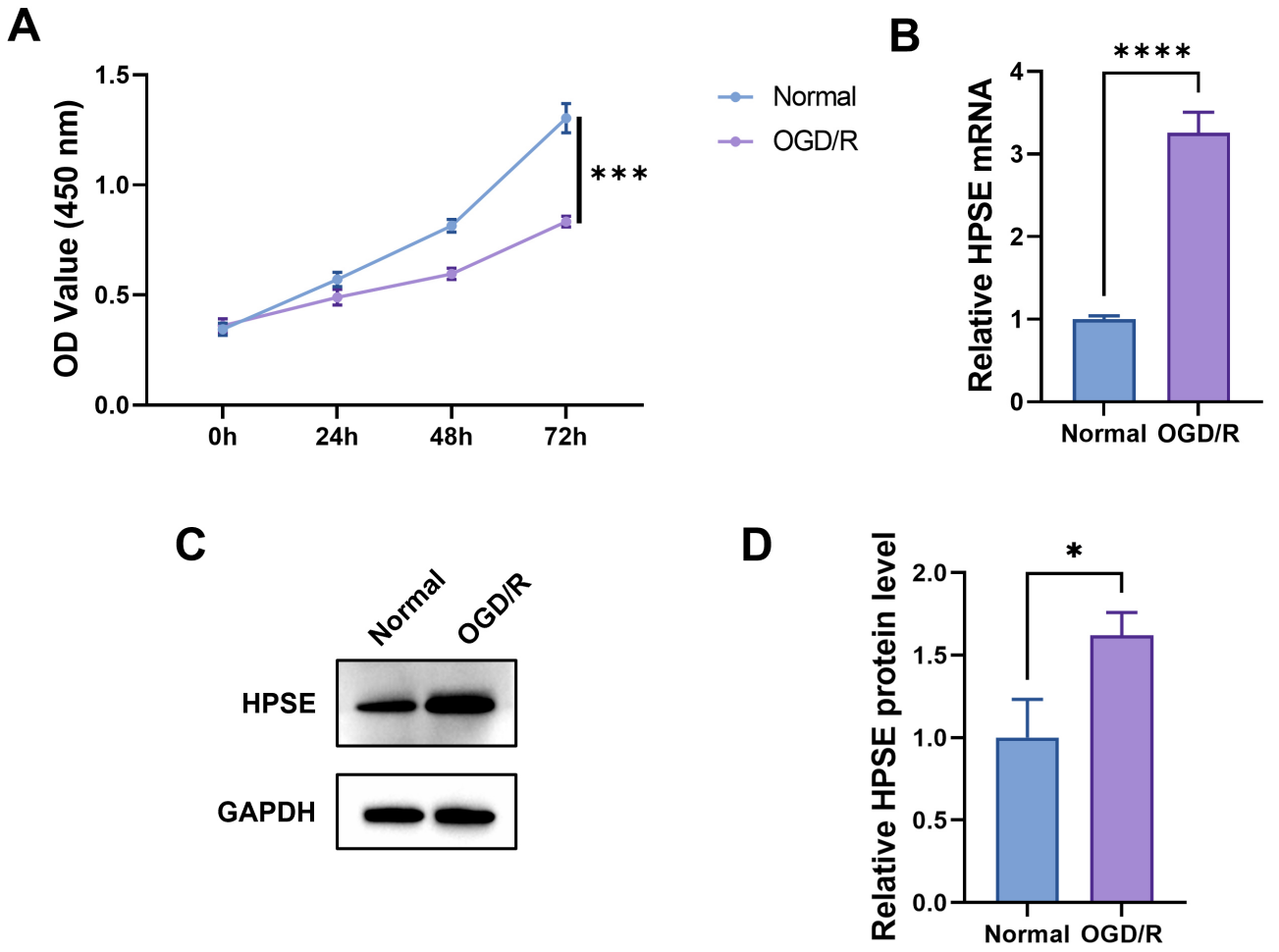

Fig. 1. HPSE was highly expressed in the OGD/R model. (A) H9c2 cells were incubated in an anaerobic chamber for 2 h, reoxygenated for 12 h, and then collected for Cell Counting Kit-8 (CCK8) assay. The relative mRNA expression levels (B) and protein levels (C) of HPSE in H9c2 cells in the OGD/R injury model were determined using qRT-PCR and western blot analysis. (D) Light density assessment of proteins detected in (C). Glyceraldehyde-3-phosphate dehydrogenase (GAPDH) was used as a loading control. N = 3. * indicates $p < 0.05$, *** indicates $p < 0.001$, **** indicates $p < 0.0001$. HPSE, heparanase; OGD/R, oxygen-glucose deprivation/reoxygenation.

OGT2115 Inhibited the Expression of Inflammatory Factors TNF-α, IL-6, and IL-8 in the OGD/R Model

The secretion of inflammatory factors plays an important role in the OGD/R injury model. We detected the secretion of TNF-α, IL-6, and IL-8 using ELISA experiments. The ELISA experiments revealed that the OGD/R injury model significantly promoted the secretion of TNF-α, IL-6, and IL-8. However, OGT2115 significantly and concentration-dependently reduced the release of TNF-α, IL-6, and IL-8 from the cells in the OGD/R injury model (Fig. 4).

OGT2115 Inhibited the Phosphorylation of MAPK and ERK

The research has demonstrated that activation of the MAPK/ERK pathway can enhance the fibrosis of cardiomyocytes, and HPSE can induce activation of the MAPK/ERK pathway. We hypothesized that OGT2115 could mitigate myocardial infarction by inhibiting the MAPK pathway. The WB experiments revealed that the OGD/R injury model did not affect the expression of P38 MAPK and ERK1/2 but significantly promoted the phosphorylation of P38 MAPK and ERK1/2 in the cells. Administration of OGT2115 did not affect the expression of P38 MAPK and ERK1/2 but significantly inhibited the phosphorylation of P38 MAPK and ERK1/2 in the cells in the OGD/R injury model in a concentration-dependent manner (Fig. 5). Taken together, OGT2115 ameliorated myocardial infarction by inhibiting the activation of the MAPK/ERK pathway.

Discussion

The leading cause of disability and mortality globally is acute myocardial infarction brought on by coronary occlusion [16]. Heart failure (HF) and ventricular remod-

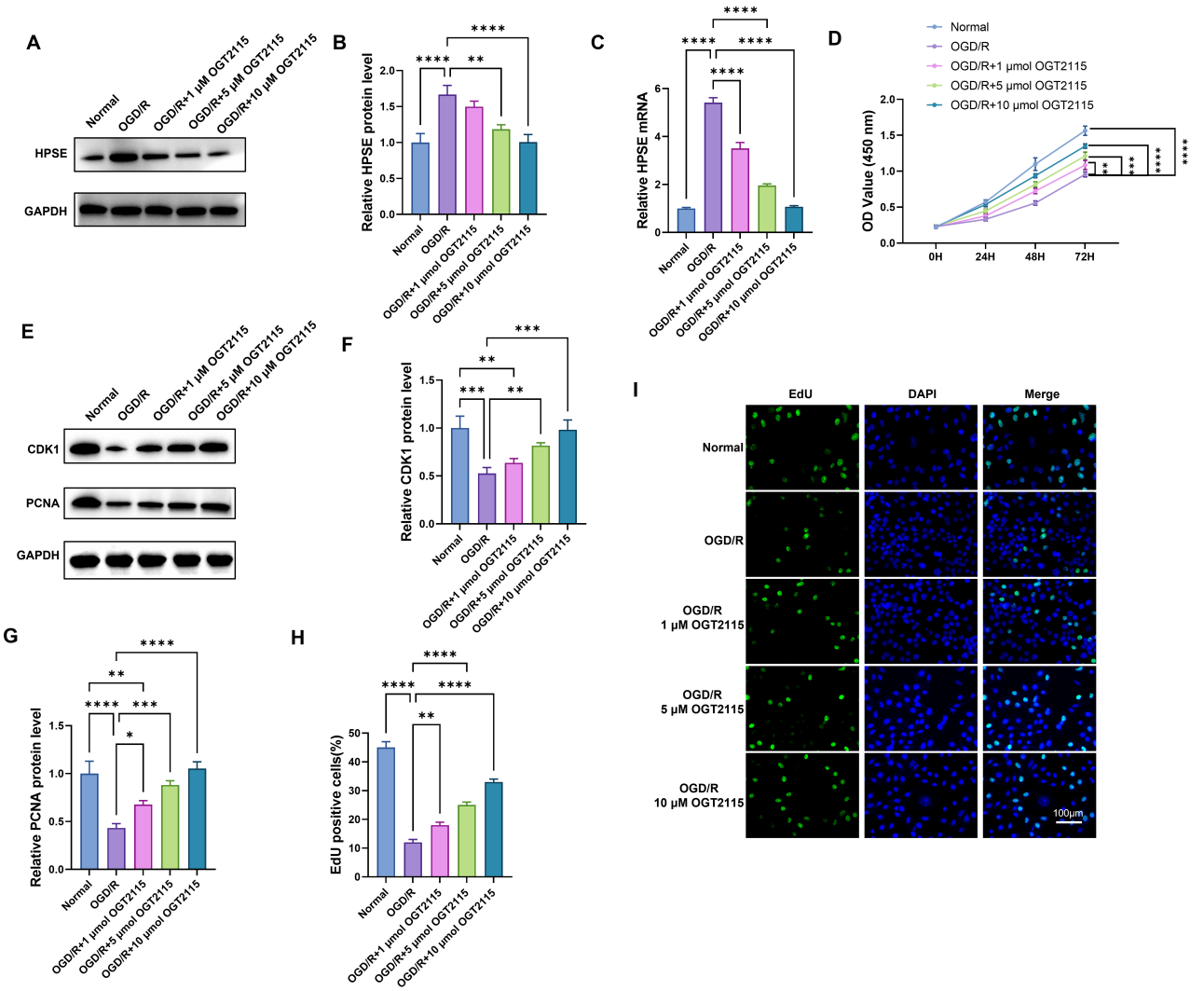

Fig. 2. The HPSE inhibitor OGT2115 significantly promoted the proliferation of H9c2 cells in the OGD/R model. The protein levels (A) and relative mRNA expression levels (C) of HPSE in H9c2 cells in OGD/R injury model in the presence of various OGT2115 concentrations (0, 1, 5, 10 μM) were determined by western blot and qRT-PCR analysis. (B) Light density assessment of proteins detected in (A). GAPDH was used as a loading control. (D) The cell viability of H9c2 cells in the OGD/R injury model at various OGT2115 concentrations (0, 1, 5, and 10 μM) for 48 h were detected using the CCK8 assay. (E) The relative protein levels of CDK1, PCNA, and GAPDH in H9c2 cells in the OGD/R injury model at various OGT2115 concentrations (0, 1, 5, and 10 μM) for 48 h were determined using western blot analysis. (G) Light density assessment of proteins detected in (E). GAPDH was used as a loading control. (H) Quantification of the 5-Ethynyl-2′-Deoxyuridine (EdU)-positive cells of (F). (I) The cell proliferation of H9c2 cells in the OGD/R injury model at various OGT2115 concentrations (0, 1, 5, and 10 μM) for 48 h were detected using the EdU staining assay. N = 3. * indicates $p < 0.05$, ** indicates $p < 0.01$, *** indicates $p < 0.001$, **** indicates $p < 0.0001$.

eling are caused by the massive death of cardiomyocytes brought on by MI, which is replaced by fibrous scar tissue [17]. Reperfusion therapy is the primary line of treatment for MI patients to save the ischemic myocardium and reduce the infarct size. However, doing so causes additional damage known as ischemia/reperfusion (I/R) injury [18]. HPSE is associated with physiological processes such as apoptosis, fibrosis, and inflammation [19]. In the present study, we explored the potential role of HPSE in acute cardiac OGD/R injury and further investigated the cardioprotective mechanism of HPSE inhibitor OGT2115. Our findings demonstrate that OGT2115 significantly reverses OGD/R-induced cytotoxicity and prevents acute cardiac OGD/R injury, thereby providing potential strategies for treating MI/R injury.

Notably, HPSE's role in developing heart-related diseases has not been investigated. In this study, we first demonstrated that HPSE was highly expressed in the OGD/R model and that the HPSE inhibitor OGT2115 was protective against acute cardiac MI/R. The experimental re-

Journal of
BIOLOGICAL REGULATORS
and Homeostatic Agents

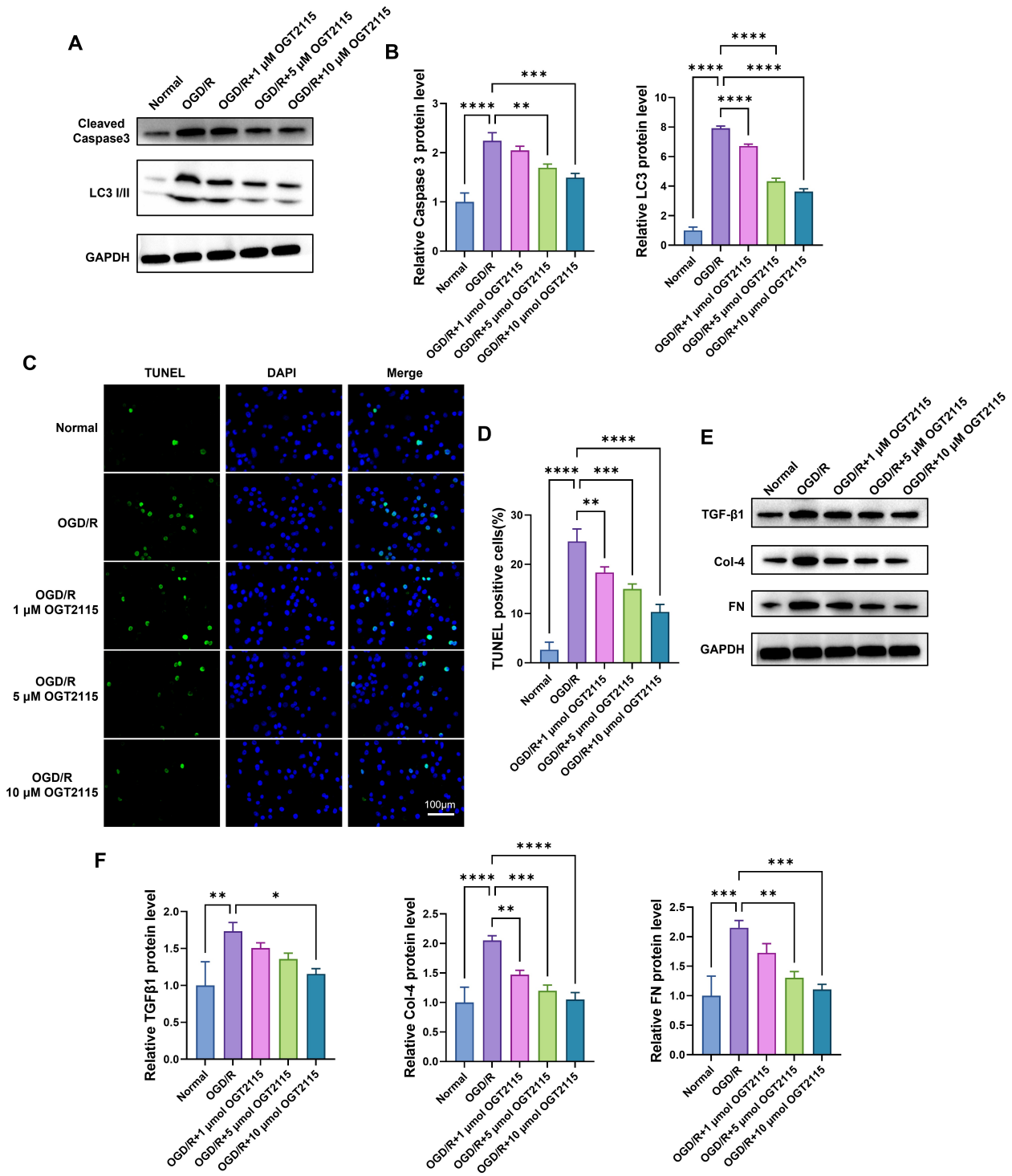

Fig. 3. The HPSE inhibitor OGT2115 significantly inhibited the apoptosis and fibrosis of H9c2 cells in the OGD/R model. (A) The relative protein levels of Caspase 3, LC3 I/II, and GAPDH in H9c2 cells in the OGD/R injury model at various OGT2115 concentrations (0, 1, 5, and 10 μM) for 48 h were determined using western blotting. (B) Light density assessment of proteins detected in (A). GAPDH was used as a loading control. (C) The cell apoptosis of H9c2 cells in the OGD/R injury model at various OGT2115 concentrations (0, 1, 5, and 10 μM) for 48 h were detected using the TdT-mediated dUTP nick-end labeling (TUNEL) staining assay. (D) Quantification of the TUNEL positive cells of (C). (E) The relative protein levels of transforming growth factor β1 (TGF-β1), collagen IV (Col-4), fibronectin (FN), and GAPDH in H9c2 cells in the OGD/R injury model at various OGT2115 concentrations (0, 1, 5, and 10 μM) for 48 h were determined using western blotting. (F) Light density assessment of proteins detected in (A). GAPDH was used as a loading control. N = 3. * indicates $p < 0.05$, ** indicates $p < 0.01$, *** indicates $p < 0.001$, **** indicates $p < 0.0001$.

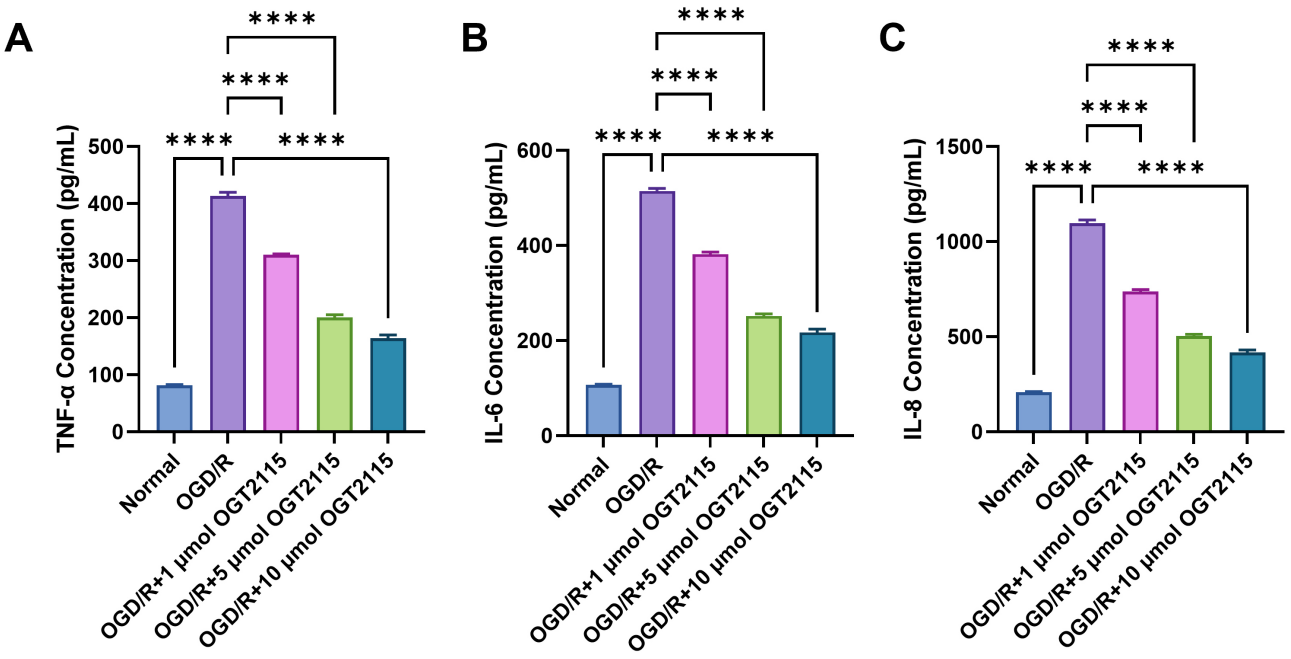

Fig. 4. OGT2115 inhibited the expression of inflammatory factors tumor necrosis factor-α (TNF-α), interleukin-6 (IL-6), and IL-8 in the OGD/R model. The concentration of TNF-α (A), IL-6 (B), and IL-8 (C) in H9c2 cells in the OGD/R injury model at various OGT2115 concentrations (0, 1, 5, and 10 μM) for 48 h were determined using the enzyme-linked immunosorbent assay (ELISA). N = 3. **** indicates $p < 0.0001$.

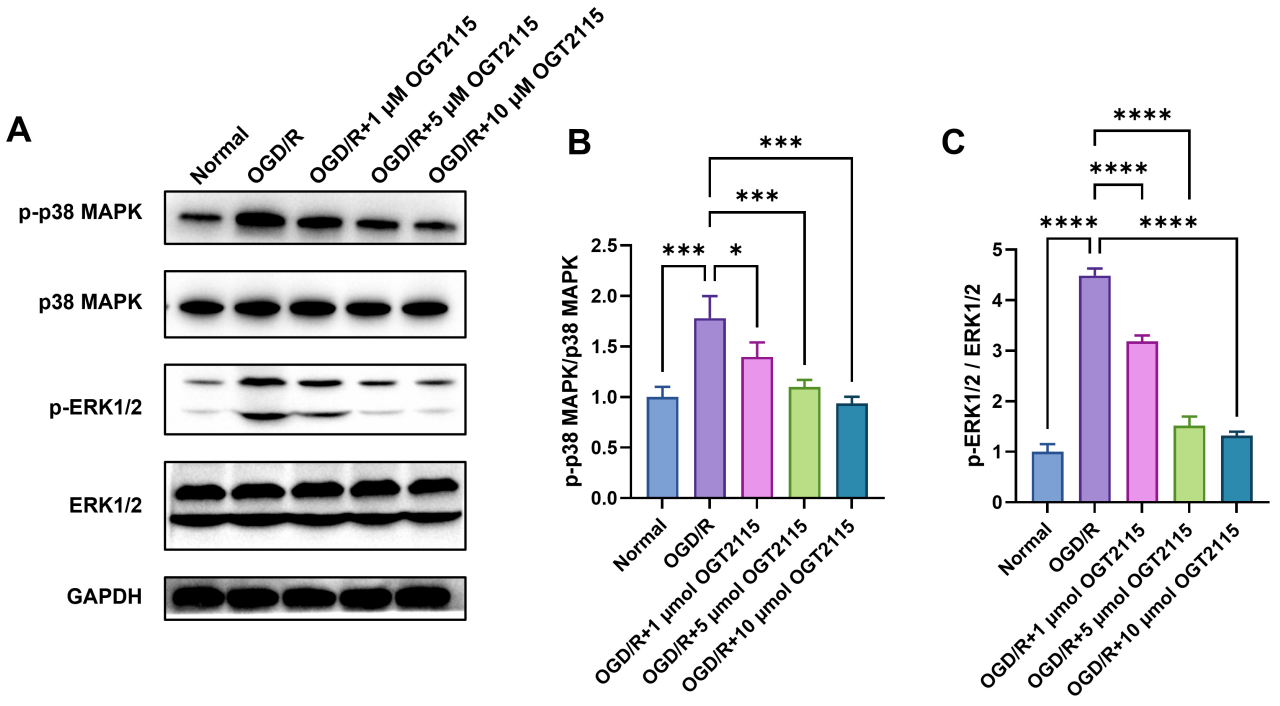

Fig. 5. OGT2115 inhibited the phosphorylation of mitogen-activated protein kinases (MAPK) and extracellular signal-regulated kinase (ERK). (A) The protein levels of p-p38 MAPK, p38 MAPK, p-ERK1/2, ERK1/2, and GAPDH in H9c2 cells in the OGD/R injury model at various OGT2115 concentrations (0, 1, 5, and 10 μM) for 48 h were determined using western blotting. (B) The ratio of p-p38 MAPK to p38 MAPK of (A). (C) The ratio of p-ERK1/2 to ERK1/2 of (A). N = 3. * indicates $p < 0.05$, *** indicates $p < 0.001$, **** indicates $p < 0.0001$.

Journal of
BIOLOGICAL REGULATORS
and Homeostatic Agents

sults indicated that OGT2115 could attenuate the decrease in cell viability and apoptosis induced by OGD/R. We further revealed that OGT2115 attenuated OGD/R-induced cardiomyocyte fibrosis and inflammation. These findings suggest that HPSE may be a therapeutic target for ischemic heart disease after reperfusion injury and deserves further study.

Study has revealed that p38 suppression improves cardiac function after MI/R by diminishing cardiomyocyte apoptosis [20]. Apoptotic mechanisms dependent on mitochondria are thought to be proximal effectors of key MAPK signaling pathway members [21]. A large body of evidence indicates that the MAPK signal transduction pathway is involved in cardiomyocyte apoptosis [22–24]. In cells under oxidative stress, the p38-MAPK pathway is activated, leading to the upregulation of BH3-only proteins, such as Bim and Bid, triggering mitochondria-dependent apoptosis pathways [25]. The ERK signaling pathway is the most studied MAPK-related pathway that regulates various biological processes, such as the survival, growth, and death of various cells and immune responses associated with inflammation [26]. Studies have demonstrated that inhibition of the ERK pathway enhances cardiomyocyte reoxygenation and inhibits apoptosis and inflammatory responses. The p-ERK/ERK ratio was increased in a rat model of AMI [27]. Meanwhile, Astragaloside IV can effectively inhibit the hyperphosphorylation of ERK, which protects the myocardium to some extent from secondary damage caused by ischemia-reperfusion [28]. This result is also consistent with our experimental results. The MAPK/ERK signaling pathway is inhibited by OGT2115, which substantially inhibits the phosphorylation of p38-MAPK and ERK. OGD/R significantly increases the phosphorylation of p38-MAPK and ERK.

This study had some limitations. *In vivo* tests are still required to confirm OGT2115's protective influence on the heart. More clinical trials are necessary to determine how OGT2115 can treat cardiovascular-related diseases.

Conclusion

In conclusion, our findings suggest that the HPSE inhibitor OGT2115 can protect myocardial tissue from OGD/R-induced cardiotoxicity by inhibiting the activation of the MAPK/ERK signaling pathway. This research may expand current techniques for preventing cardiomyocyte I/R damage in the early stages of reperfusion and offer fresh approaches for treating ischemic heart disease. These findings may broaden existing techniques for preventing cardiomyocyte I/R damage during the early stages of reperfusion and provide novel approaches for treating ischemic heart diseases.

Availability of Data and Materials

All data generated or analyzed during this study are included in this article. Further inquiries can be directed to the corresponding author.

Author Contributions

YX and HL provided the experimental design; HL, YZ, and DG performed the experiments; HL and GX analyzed the data; YX and HL prepared all figures, and YX and HL wrote the draft of the manuscript. All authors reviewed the manuscript. All authors have contributed to the creation of the manuscript and approved to submit it to the journal. All authors contributed to editorial changes in the manuscript. All authors read and approved the final manuscript. All authors have participated sufficiently in the work and agreed to be accountable for all aspects of the work.

Ethics Approval and Consent to Participate

Not applicable.

Acknowledgment

Not applicable.

Funding

This work was supported by the Ningbo Natural Science Foundation of China (2018A610393).

Conflict of Interest

The authors declare no conflict of interest.

References

[1] Li P, Ge J, Li H. Lysine acetyltransferases and lysine deacetylases as targets for cardiovascular disease. Nature Reviews. Cardiology. 2020; 17: 96–115.

[2] Thygesen K, Alpert JS, Jaffe AS, Chaitman BR, Bax JJ, Morrow DA, *et al*. Fourth Universal Definition of Myocardial Infarction (2018). Journal of the American College of Cardiology. 2018; 72: 2231–2264.

[3] Wereski R, Kimenai DM, Bularga A, Taggart C, Lowe DJ, Mills NL, *et al*. Risk factors for type 1 and type 2 myocardial infarction. European Heart Journal. 2022; 43: 127–135.

[4] Cahill TJ, Choudhury RP, Riley PR. Heart regeneration and repair after myocardial infarction: translational opportunities for novel therapeutics. Nature Reviews. Drug Discovery. 2017; 16: 699–717.

[5] Ozaki Y, Hara H, Onuma Y, Katagiri Y, Amano T, Kobayashi Y, *et al*. CVIT expert consensus document on primary percutaneous coronary intervention (PCI) for acute myocardial infarction (AMI) update 2022. Cardiovascular Intervention and Therapeutics. 2022; 37: 1–34.

[6] Lu S, Tian Y, Luo Y, Xu X, Ge W, Sun G, *et al*. Iminostilbene, a novel small-molecule modulator of PKM2, suppresses

macrophage inflammation in myocardial ischemia-reperfusion injury. Journal of Advanced Research. 2020; 29: 83–94.

[7] Han D, Wang Y, Chen J, Zhang J, Yu P, Zhang R, *et al*. Activation of melatonin receptor 2 but not melatonin receptor 1 mediates melatonin-conferred cardioprotection against myocardial ischemia/reperfusion injury. Journal of Pineal Research. 2019; 67: e12571.

[8] Wang R, Wang M, He S, Sun G, Sun X. Targeting Calcium Homeostasis in Myocardial Ischemia/Reperfusion Injury: An Overview of Regulatory Mechanisms and Therapeutic Reagents. Frontiers in Pharmacology. 2020; 11: 872.

[9] Wu L, Davies GJ. An Overview of the Structure, Mechanism and Specificity of Human Heparanase. Advances in Experimental Medicine and Biology. 2020; 1221: 139–167.

[10] Koganti R, Suryawanshi R, Shukla D. Heparanase, cell signaling, and viral infections. Cellular and Molecular Life Sciences. 2020; 77: 5059–5077.

[11] Simeonovic CJ, Ziolkowski AF, Wu Z, Choong FJ, Freeman C, Parish CR. Heparanase and autoimmune diabetes. Frontiers in Immunology. 2013; 4: 471.

[12] Ostrovsky O, Vlodavsky I, Nagler A. Mechanism of HPSE Gene SNPs Function: From Normal Processes to Inflammation, Cancerogenesis and Tumor Progression. Advances in Experimental Medicine and Biology. 2020; 1221: 231–249.

[13] Secchi MF, Masola V, Zaza G, Lupo A, Gambaro G, Onisto M. Recent data concerning heparanase: focus on fibrosis, inflammation and cancer. Biomolecular Concepts. 2015; 6: 415–421.

[14] Courtney SM, Hay PA, Buck RT, Colville CS, Phillips DJ, Scopes DIC, *et al*. Furanyl-1,3-thiazol-2-yl and benzoxazol-5-yl acetic acid derivatives: novel classes of heparanase inhibitor. Bioorganic & Medicinal Chemistry Letters. 2005; 15: 2295–2299.

[15] Deng Z, Ou H, Ren F, Guan Y, Huan Y, Cai H, *et al*. LncRNA SNHG14 promotes OGD/R-induced neuron injury by inducing excessive mitophagy via miR-182-5p/BINP3 axis in HT22 mouse hippocampal neuronal cells. Biological Research. 2020; 53: 38.

[16] Wu X, Reboll MR, Korf-Klingebiel M, Wollert KC. Angiogenesis after acute myocardial infarction. Cardiovascular Research. 2021; 117: 1257–1273.

[17] Kapur NK, Thayer KL, Zweck E. Cardiogenic Shock in the Setting of Acute Myocardial Infarction. Methodist DeBakey Cardiovascular Journal. 2020; 16: 16–21.

[18] Rout A, Tantry US, Novakovic M, Sukhi A, Gurbel PA. Targeted pharmacotherapy for ischemia reperfusion injury in acute myocardial infarction. Expert Opinion on Pharmacotherapy. 2020; 21: 1851–1865.

[19] Ostrovsky O, Baryakh P, Morgulis Y, Mayorov M, Bloom N, Beider K, *et al*. The HPSE Gene Insulator-A Novel Regulatory Element That Affects Heparanase Expression, Stem Cell Mobilization, and the Risk of Acute Graft versus Host Disease. Cells. 2021; 10: 2523.

[20] Xie D, Zhao J, Guo R, Jiao L, Zhang Y, Lau WB, *et al*. Sevoflurane Pre-conditioning Ameliorates Diabetic Myocardial Ischemia/Reperfusion Injury Via Differential Regulation of p38 and ERK. Scientific Reports. 2020; 10: 23.

[21] Wagner EF, Nebreda AR. Signal integration by JNK and p38 MAPK pathways in cancer development. Nature Reviews. Cancer. 2009; 9: 537–549.

[22] Yang C, Zeng X, Cheng Z, Zhu J, Fu Y. Aconitine Induces TRPV2-Mediated Ca^{2+} Influx through the p38 MAPK Signal and Promotes Cardiomyocyte Apoptosis. Evidence-Based Complementary and Alternative Medicine. 2021; 2021: 9567056.

[23] Guo W, Liu X, Li J, Shen Y, Zhou Z, Wang M, *et al*. Prdx1 alleviates cardiomyocyte apoptosis through ROS-activated MAPK pathway during myocardial ischemia/reperfusion injury. International Journal of Biological Macromolecules. 2018; 112: 608–615.

[24] Oh CC, Lee J, D'Souza K, Zhang W, Migrino RQ, Thornburg K, *et al*. Activator protein-1 and caspase 8 mediate p38α MAPK-dependent cardiomyocyte apoptosis induced by palmitic acid. Apoptosis. 2019; 24: 395–403.

[25] Cuadrado A, Nebreda AR. Mechanisms and functions of p38 MAPK signalling. The Biochemical Journal. 2010; 429: 403–417.

[26] Sun Y, Liu WZ, Liu T, Feng X, Yang N, Zhou HF. Signaling pathway of MAPK/ERK in cell proliferation, differentiation, migration, senescence and apoptosis. Journal of Receptor and Signal Transduction Research. 2015; 35: 600–604.

[27] Liu X, Gu J, Fan Y, Shi H, Jiang M. Baicalin attenuates acute myocardial infarction of rats via mediating the mitogen-activated protein kinase pathway. Biological & Pharmaceutical Bulletin. 2013; 36: 988–994.

[28] Wu Y, Fan Z, Chen Z, Hu J, Cui J, Liu Y, *et al*. Astragaloside IV protects human cardiomyocytes from hypoxia/reoxygenation injury by regulating miR-101a. Molecular and Cellular Biochemistry. 2020; 470: 41–51.